Influence of key residues on the heterologous extracellular production of fungal ribonuclease U2 in the yeast *Pichia pastoris*.

Elisa Álvarez-García[a], Lucía García-Ortega[a], Vivian De los Ríos[b], José G. Gavilanes[a]*, Álvaro Martínez-del-Pozo[a]*

[a]Departamento de Bioquímica y Biología Molecular I, Facultad de Ciencias Químicas, Universidad Complutense, Avenida Complutense s/n, Ciudad Universitaria, 28040 Madrid, Spain.
[b]Centro de Investigaciones Biológicas – C.S.I.C., Ramiro de Maeztu 9, 28040 Madrid, Spain

**Corresponding authors:* JGG (ppgf@bbm1.ucm.es) and AMP (alvaro@bbm1.ucm.es). Fax: 34-91-394-4159

Short title: Key residues in the production of ribonuclease U2

Abstract

Ribonuclease U2, secreted by the smut fungus *Ustilago sphaerogena*, is a cyclizing ribonuclease that displays a rather unusual specificity within the group of microbial extracellular RNases, best represented by RNase T1. Superposition of the three-dimensional structures of RNases T1 and U2 suggests that the RNase U2 His 101 would be the residue equivalent to the RNase T1 catalytically essential His 92. RNase U2 contains three disulfide bridges but only two of them are conserved among the family of fungal extracellular RNases. The non-conserved disulfide bond is established between Cys residues 1 and 54. Mispairing of the disulfide network due to the presence of two consecutive Cys residues (54 and 55) has been invoked to explain the presence of wrongly folded RNase U2 species when produced in *P. pastoris*. In order to study both hypotheses, the RNase U2 H101Q and C1/54S variants have been produced, purified, and characterized. The results obtained support the major conclusion that His 101 is required for proper protein folding when secreted by the yeast *P. pastoris*. On the other hand, substitution of the first Cys residue for Ser results in a mutant version which is more efficiently processed in terms of a more complete removal of the yeast α-factor signal peptide. In addition, it has been shown that elimination of the Cys 1-Cys 54 disulfide bridge does not interfere with RNase U2 proper folding, generating a natively folded but much less stable protein.

Keywords: microbial ribonucleases, RNase T1, fungal ribonucleases, disulfide.

Introduction

Ribonuclease U2 (RNase U2) is a single polypeptide chain enzyme of 114 amino acid residues secreted by the smut fungus *Ustilago sphaerogena* [1-4]. This cyclizing ribonuclease displays a rather unusual specificity within the group of microbial extracellular RNases, best represented by RNase T1 [5-7], showing a strong preference for 3'-linked purine phosphodiester linkages [8]. This unique specificity converts RNase U2 in a very useful biotechnological tool of increasing importance regarding RNA sequencing and processing [9-11]. Indeed, this enzyme is the fungal non-toxic RNase which appears to be the phylogenetically closest relative of ribotoxins, a family of highly specific ribosome-inactivating fungal proteins with antitumoral properties [12]. Therefore, RNase U2 is the best model to compare the mechanisms of both toxic and non-toxic groups of microbial RNases. Nevertheless, all these extracellular fungal RNases of the RNase T1 family, ribotoxins included, share an identical structural core [12-15] and comparison of their three-dimensional structures reveals that they have equivalent regular secondary structure elements, as well as an almost identical spatial arrangement of the residues involved in the active site (Fig. 1). Superposition of these structures suggests that the RNase U2 residue equivalent to RNase T1 catalytically essential His 92 [5] would be His 101 [13,16] (Fig. 1). With the purpose of verifying this hypothesis, this potentially catalytic His 101 has been replaced by a Gln residue and the resulting mutant protein has been purified and characterized.

Besides being a small enzyme, RNase U2 also shows a good number of unusual structural attributes which may be related to its particular specificity and mode of action. For example, one of its most distinctive features is the absence of any Lys residue and the presence of just a single Arg, what results in a highly acidic pI value of about 3.0 [1,17,18], and an anomalous electrophoretic behavior, even in the presence of SDS [19]. It is also a peculiar protein from a spectroscopic point of view since it contains a single but strongly quenched Trp residue [20,21]. Natural wild-type RNase U2 in solution is slowly converted upon ageing into two other isoforms containing one or two isoaspartate bonds

and different secondary structure and specific enzymatic activity [17,21-23]. Finally, RNase U2 contains three disulfide bridges being only two of them conserved among most of the fungal extracellular RNases known [4,24]. Interestingly, the non-conserved one is established between Cys 1 and Cys 54, contiguous to Cys 55, also involved in another bridge with Cys 96 [1,25]. Mispairing of the disulfide network due to the presence of these two consecutive Cys residues (54 and 55) has been invoked to explain the presence of two isoforms upon recombinant production of RNase U2 in the yeast *Pichia pastoris* [4,21]. In the present work this hypothesis has been also further explored through production, purification, and characterization of a double mutant where both Cys residues 1 and 54 have been replaced by Ser.

Materials and methods

DNA Manipulations

All of the materials and reagents were of molecular biology grade. Cloning procedures and bacteria manipulations were carried out according to standard methods [26], as described previously [27,28]. *In vitro* site-directed mutagenesis using a double-stranded DNA template and two oligonucleotides annealing to the complementary strands was used to obtain the mutants as described [26]. Two different mutants were constructed: A single one where His 101 was replaced by Gln (H101Q) and a double one where Cys 1 and 54 were both substituted by Ser (C1/54S). The template employed was the plasmid pPICZαU2, used before to produce the wild-type protein in *P. pastoris* [19], or that one corresponding to the mutated Cys 1 for the double mutant. These plasmids confer resistance to the antibiotic zeocin. The mutagenic primers used are shown in Table 1. PCR amplification of the mutagenic mixture was performed in standard conditions using a mixture of Taq-Gold and Vent DNA polymerases and the Taq-extender buffer to complete the copy of the entire lengths of both template complementary DNA strands. Selection of mutants was achieved after treatment with DpnI, which specifically cleaves methylated

sequences [29]. The expression constructs were obtained using the *Escherichia coli* strain DH5αF' [26-28,30]. Presence of only the mutations expected in each case was confirmed by sequencing the complete cloned cDNA at the Universidad Complutense DNA-Sequencing Facility.

Production and purification of the proteins

P. pastoris GS115 or KM71 cells carrying the corresponding plasmids were screened as described [19,21,31]. The appropriate clones were first selected on zeocin-containing agar plates and then through small-scale production experiments. Large-scale production of the recombinant proteins was carried out in buffered minimal medium as described [19,21]. The extracellular media of the corresponding cultures were exhaustively dialyzed against 20 mM piperazine, pH 6.0, and then loaded onto DEAE-cellulose equilibrated in the same buffer. The protein was eluted in each case with a 0-0.5 M NaCl linear gradient. Fractions containing the wild-type RNase U2 or its mutant variants were pooled, dialyzed against 50 mM sodium acetate, pH 4.5, and chromatographied on a 2',5'-ADP-Sepharose (Pharmacia) column, which acts as an affinity bed for fully active RNase U2 [21]. Proteins were finally eluted with a linear gradient, 50 mM sodium acetate (pH 4.5)/50 mM Tris-HCl (pH 7.0) containing 50 mM NaCl. When purifying the H101Q mutant, volume excluded from the affinity column was also collected, concentrated, and further fractionated by means of a gel filtration step on a Bio-Gel P10 column (2 x 150 cm) equilibrated in 50 mM Tris-HCl, pH 7.0, containing 0.1 M NaCl. After both chromatographic steps, fractions containing the mutant RNases U2 were finally pooled, concentrated, dialyzed against 50 mM ammonium acetate, pH 4.5, and lyophilized.

Electrophoretic and chemical characterization

Given the particular electrophoretic behavior of RNase U2, polyacrylamide gel electrophoresis and Western blots were performed as described before [19]. Glycoproteins and glycopeptides were detected with biotinylated-Con A lectin following a standard procedure [32,33]. Protein

hydrolysis and amino acid analysis were performed according to standard procedures [27,34]. These analyses were employed to estimate extinction coefficients ($E^{0.1\%}$) and protein concentrations (Table 2). Immunodetection of the blotted proteins was performed with a rabbit polyclonal sera raised against purified recombinant wild-type RNase U2 [19].The amino-terminal sequences were determined by Edman degradation using an Applied Biosystems model 477A sequencer at the C.I.B.-C.S.I.C. (Madrid, Spain) Protein Sequencing Facility.

Spectroscopic characterization

Absorbance measurements were performed on an Uvikon 930 spectrophotometer at 100 nm/min scanning speed, at room temperature and in 1 cm optical path cells. Circular dichroism (CD) spectra were obtained on a Jasco 715 spectropolarimeter, equipped with a thermostated cell holder and a NesLab-111 circulating water bath, at 0.2 nm/s scanning speed. The instrument was calibrated with (1)-10-camphorsulfonic acid. CD spectra were recorded in cylindrical cells of 0.1 cm optical path. Mean residue weight ellipticities were expressed in units of degree x cm^2 x $dmol^{-1}$. Thermal denaturation profiles were obtained by measuring the temperature dependence of the ellipticity at 220nm in the 25–85ºC range. The temperature was continuously changed at a rate of 0.5ºC/min. Tm (temperature at the midpoint of the thermal transition) values were calculated assuming a two-state unfolding mechanism [35]. Fluorescence emission spectra were recorded on an SLM Aminco 8000 spectrofluorimeter at 25ºC using a slit width of 4 nm for both excitation and emission beams. The spectra were recorded for excitation at 275 and 295 nm and both were normalized by considering that Tyr emission above 380 nm is negligible. The Tyr contribution was calculated as the difference between the two normalized spectra. Thermostated cells with a path length of 0.2 and 1.0 cm for the excitation and emission beams, respectively, were used. The temperature was controlled by a circulating water bath. All these experiments were performed with the proteins dissolved in 50 mM sodium acetate pH 4.5.

Mass spectrometry

Protein samples were analyzed as described before [19] on an Autoflex III MALDI-TOF-TOF instrument (Bruker Daltonics, Bremen, Germany) with a smartbeam laser. The spectra were acquired using a laser power just above the ionization threshold. Samples were analysed in the positive ion detection and delayed extraction linear mode. Typically, 1000 laser shots were summed into a single mass spectrum. External calibration was performed, using the Protein Calibration I from Bruker, covering the range from 5000 to 17000 Da. The 2,5-dihydroxy-acetophenone (2,5-DHAP) matrix solution was prepared by dissolving 7.6 mg (50 µmol) in 375 µl ethanol followed by the addition of 125 µl of 80 mM diammonium hydrogen citrate aqueous solution. For sample preparation, 2.0 µl of the sample were diluted with 2.0 µl of 2% trifluoro acetic acid aqueous solution and 2.0 µl of matrix solution. A volume of 1.0 µl of this mixture was spotted onto the stainless steel target and allowed to dry at room temperature.

Ribonucleolytic Activity.

The activity of the purified proteins was assayed by using a zymogram against poly (A) in 15% (w/v) polyacrylamide gels containing 0.1% (w/v) SDS and 0.3 mg/ml of the homopolynucleotide as previously described [19,27,28,30,36-38]. After electrophoresis, the gel was washed to eliminate the SDS, incubated at pH 4.5 for 1.5 h at 37 °C, and then stained with 0.2% (w/v) toluidine blue. The proteins exhibiting ribonuclease activity appear as colorless bands, because of degradation of the polynucleotide, after appropriate distaining. This assay is also useful to detect the presence of other RNA degrading activities in the protein samples. Volumograms of these bands (based on integrating all of the pixel intensities composing the spot) were obtained with the photo documentation system UVI-Tec (Cambridge, UK) and the software facility UVIsoft UVI band Windows Application V97.04 [19,27,28,30,38]. These data were used to quantify the activity (Table 3).

Results and Discussion

Protein production and purification

In order to study the potentially catalytic role of His 101, the RNase U2 H101Q mutant was prepared, produced in *P. pastoris* and purified. Unexpectedly, no 2',5'-ADP-Sepharose binding fraction was detected but rather all the mutant protein appeared in the void volume of the column, according to its electrophoretic and immunogenic behavior (Fig. 2). This affinity chromatography step was introduced previously [4,21], when first purifying the recombinant wild-type RNase U2, in order to remove a presumably misfolded fraction of the protein with an apparent Trp fluorescence. However, now the production of H101Q in identical conditions rendered only a protein fraction unable to bind to the affinity column. The 2',5'-ADP ligand should still be recognized if the active site geometric arrangement was being preserved in the mutant. In fact, substitution of the equivalent His residue in other fungal extracellular RNases has resulted in inactive mutant proteins which still retained the native conformation [28,39]. So, this result suggested a misfolded conformation of the H101Q mutant to explain its inability to bind to the column. In order to confirm this suggestion, this excluded protein fraction was further fractionated by means of a gel filtration column, pooled and characterized (Table 2).

Cysteine pairing isomerism involving Cys residues 1, 54, 55 and 96 has been invoked to explain the presence of a misfolded wild-type RNase U2 fraction within the extracellular media of *P. pastoris* cells harboring the pPICZαU2 plasmid [4,21]. Given the result obtained upon purification of the H101Q mutant, and now in order to study the role of the non-conserved disulfide bridge, the RNase U2 C1/54S double mutant was also produced and purified (Fig. 2). In this case, the mutant did bind to the column with no immunoreactive protein detected in the excluded fractions, suggesting that only a properly folded protein fraction was being produced, with a very similar yield than in the case of the wild-type RNase U2 (Table 2).

Structural characterization

Amino acid analyses matched those ones expected according to their cDNA-deduced amino acid sequences (data not shown). Furthermore, both protein mutants isolated were purified to electrophoretic homogeneity (Fig. 2). RNase U2 does not bind SDS under the SDS-PAGE conditions, its electrophoretic mobility being only determined by its electrostatic charge and hydrodynamic properties. Accordingly, the C1/54S mutant, lacking one disulfide bridge, exhibited a lower mobility when applied under non-reducing conditions (Fig. 3), suggesting a more relaxed conformation. In both cases studied the presence of a predominant immunoreactive band was evident confirming that a protein with the RNase U2 polypeptide primary structure was the main component in the purified preparations (Fig. 2).

In wild-type RNase U2, Cys 1 impairs proper proteolytic processing of the yeast α-factor signal peptide artificially fused to the RNase U2 sequence when produced in *P. pastoris* (Fig. 4). This fact explains why the recombinant wild-type protein still retains six amino acids belonging to that signal peptide (Fig. 4 and Table 2) [16,18]. Amino-terminal sequencing revealed the presence of at least three different sequences for the H101Q sample (Table 2), corresponding to three different sites of signal-peptide proteolytic processing (Fig. 4), and confirming the inefficiency of this cleavage which is indeed heterogeneous for this mutant. On the other hand, substitution of Cys 1 by Ser rendered a protein with a single amino-terminal sequence (Table 2) corresponding to a more efficient signal-peptide cleavage. Thus, only two extra residues remain in the C1/54S mutant when compared to the natural mature protein (Fig. 3). These observations were further confirmed by MALDI-TOF analyses (Fig. 5). The results obtained matched the molecular mass expected for the C1/54S protein while they were higher and more heterogeneous for the other mutant (Fig. 5), suggesting the presence of posttranslational modifications for the H101Q RNase U2 as well as the presence of small size contaminants. Heterologous protein glycosylation in *P. pastoris* is rather frequent even if that protein is not glycosylated by its native host [40,41]. Wild-type RNase U2 and the two mutants studied do not contain an Asn-glycosylation consensus sequence.

Nevertheless, it has been shown that *P. pastoris* can also add O-oligosaccharides composed of mannose to different residues of the same protein [40]. In fact, the H101Q mutant showed high degree of heterogeneous glycosylation (Fig. 3) while the wild-type and the C1/54S variant were not modified in identical culture conditions. Interestingly, the substituted His 101 is flanked by two Thr residues (Thr 100 and Thr 102) that eventually might become accessible to glycosylation upon protein misfolding. Furthermore, *P. pastoris* secretes mannans at high concentration that can non-covalently associate with heterologous proteins expressed extracellularly and copurify with them [41], which may explain the presence of many of the small size contaminants observed in the H101Q MS spectrum. In good agreement with all results shown above, far-UV CD spectra of wild-type RNase U2 [19] and its C1/54S variant were indistinguishable (Fig. 6), while the H101Q mutant displayed a much different spectrum, consistent with high content of random secondary structure (Fig. 6).

One of the most distinct spectral features of RNase U2 is the low fluorescence emission above 340 nm besides the existence of a Trp residue. Consequently, the C1/54S mutant protein showed the characteristic fungal natural RNase U2 fluorescence emission spectra centered around 300 nm when excited at 275 nm (Fig. 7). On the other hand, quantum yields were much higher and Trp fluorescence emission was much more evident in the H101Q preparation (Fig. 7), as it had been observed before with the excluded protein fraction of the wild type RNase U2 [4,21], and in good agreement with a misfolded conformation.

Thermal denaturation profiles of both wild-type and C1/54S RNases U2 (Fig. 5) confirmed that the mutant protein displayed a native conformation. The absence of the disulfide bridge was however evidenced by its much lower Tm values when compared to the wild-type protein (Table 2).

In summary, the structural characterization revealed that the C1/54S mutant protein, capable of binding to the 2',5'-ADP-Sepharose, exhibited the wild-type native conformation but with a much reduced thermostability and a shorter amino-terminal remain of the artificially fused signal peptide. On the

other hand, the H101Q variant was not retained by the affinity column and displayed structural and spectroscopic features that were not compatible with the natural fungal RNase U2 native conformation.

Enzymatic characterization

Zymogram assays showed that the C1/54S mutant did cleave the homopolynucleotide poly (A) to a comparable extent (60%) as the native recombinant wild-type RNase U2 at pH 4.5, a unique feature of this enzyme (Fig. 3). In agreement with the structural data discussed above, the H101Q mutant was devoid of detectable enzymatic activity when assayed under identical conditions (Fig. 3).

Conclusions

Structural comparisons suggest RNase U2 His 101 as the best candidate residue to fulfill the role of general acid during the transphosphorylation step leading to RNA cleavage. Unexpectedly, mutation of this residue by Gln strongly supports the major conclusion that this residue is essential for proper protein folding upon production in *P. pastoris*. On the other hand, the non-conserved disulfide bond very clearly influences the stability of the protein, since its elimination results in a native and fully active but less stable mutant RNase U2, as evidenced by the thermostability experiments. However, the presence of Cys 1 leads to a deficient removal of the yeast α–factor signal peptide used to induce its secretion to the extracellular medium. Both Cys 1 and 54 do also seem to allow a percentage of incorrect disulfide bridges arrangement resulting in the production of a significant amount of wild-type protein molecules exhibiting a non-native folding pattern and therefore unable to bind to the affinity column employed for their purification.

Acknowledgements

This work was supported by grant BFU2006-04404 from the Ministerio de Educación y Ciencia (Spain). E. A.-G. is recipient of a fellowship from the Ministerio de Educación y Ciencia (Spain). L.G.-O. is a *Juan de la Cierva* research fellow, a position partially funded by the European Social Foundation.

References

[1] S. Sato, T. Uchida, The amino acid sequence of ribonuclease U2 from *Ustilago sphaerogena*, Biochem. J. 145 (1975) 353-360.

[2] T. Arima, T. Uchida, F. Egami, Studies on extracellular ribonucleases of *Ustilago sphaerogena*. Purification and properties. Biochem. J. 106 (1968) 601–607.

[3] T. Arima, T. Uchida, F. Egami, Studies on extracellular ribonucleases of *Ustilago sphaerogena*. Characterization of substrate specificity with special reference to purine-specific ribonucleases. Biochem. J. 106 (1968) 609–613.

[4] A. Martínez-Ruiz, L. García-Ortega, R. Kao, J. Lacadena, M. Oñaderra, J.M. Mancheño, J. Davies, A. Martínez del Pozo, J.G. Gavilanes, RNase U2 and α-sarcin: a study of relationships. Methods Enzymol. 341 (2001) 335–351.

[5] J. Steyaert, A decade of protein engineering on ribonuclease T1-atomic dissection of the enzyme-substrate interactions. Eur. J. Biochem. 247 (1997) 1-11.

[6] H. Yoshida, The ribonuclease T1 family. Methods Enzymol. 341 (2001) 28-41.

[7] S. Loverix, J. Steyaert, Deciphering the mechanism of RNase T1. Methods Enzymol. 341 (2001) 305–323.

[8] T. Uchida, T. Arima, F. Egami, Specificity of RNase U2. J. Biochem. 67 (1970) 91-102.

[9] M. Escaffre, A. Favre, J.C. Chottard, S. Bombard. Determination of platinated purines in oligoribonucleotides by limited digestion with ribonucleases. Anal. Biochem. 310 (2002) 42-49.

[10] N.N. Singh, R.N. Singh, E.J. Androphy. Modulating role of RNA structure in alternate splicing of a critical exon in the spinal muscular atrophy genes. Nucleic Acids Res. 35 (2007) 371-389.

[11] J.S. Yu, R.J. Kokoska, V. Khernici, D.A. Steege. In-frame overlapping genes: The challenges for regulating gene expression. Molec. Microbiol. 63 (2007) 1168-1172.

[12] J. Lacadena, E. Álvarez-García, N. Carreras-Sangrà, E. Herrero-Galán, J. Alegre-Cebollada, L. García-Ortega, M. Oñaderra, J.G. Gavilanes, A. Martínez del Pozo, Fungal ribotoxins: molecular dissection of a family of natural killers. FEMS Microbiol. Rev. 31 (2007) 212-237.

[13] R. Campos-Olivas, M. Bruix, J. Santoro, A. Martínez del Pozo, J. Lacadena, J.G. Gavilanes, M. Rico, Structural basis for the catalytic mechanism and substrate specificity of the ribonuclease α-sarcin. FEBS Lett. 399 (1996) 163-165.

[14] X. Yang, K. Moffat, Insights into specificity of cleavage and mechanism of cell entry from the crystal structure of the highly specific *Aspergillus* ribotoxin, restrictocin. Structure 4 (1996) 837-852.

[15] J.M. Pérez-Cañadillas, J. Santoro, R. Campos-Olivas, J. Lacadena, A. Martínez del Pozo, J.G. Gavilanes, M. Rico, M. Bruix, The highly refined solution structure of the cytotoxic ribonuclease α-sarcin reveals the structural requirements for substrate recognition and ribonucleolytic activity. J. Mol. Biol. 299 (2000) 1061-1073.

[16] E. Herrero-Galán, J. Lacadena, A. Martínez del Pozo, D.G. Boucias, N. Olmo, M. Oñaderra, J.G. Gavilanes, The insecticidal protein hirsutellin A from the mite fungal pathogen *Hirsutella thompsonii* is a ribotoxin. Proteins 72 (2008) 217-228.

[17] S. Kanaya, T. Uchida, Comparison of the primary structures of ribonuclease U2 isoforms. Biochem. J. 240 (1986) 163-170.

[18] S. Kanaya, T. Uchida, Revised sequence of ribonuclease U2 in the substrate-binding region. J. Biochem. 118 (1995) 681–682.

[19] L. García-Ortega, V. De los Ríos, A. Martínez-Ruiz, M. Oñaderra, J. Lacadena, A. Martínez del Pozo, J.G. Gavilanes, Anomalous electrophoretic behavior of a very acidic protein: ribonuclease U2. Electrophoresis 26 (2005) 3407-3413.

[20] S. Minato, A. Hirai, Characterization of *Ustilago* Ribonuclease U2. Effects of chemical modification at glutamic acid-61 and cystine-1 and of organic solvents on the enzymatic activity. J. Biochem. 85 (1979) 327–344.

[21] A. Martínez-Ruiz, L. García-Ortega, R. Kao, M. Oñaderra, J.M. Mancheño, J. Davies, A. Martínez del Pozo, J.G. Gavilanes, Ribonuclease U2: cloning,

production in *Pichia pastoris* and affinity chromatography purification of the active recombinant protein. FEMS Microbiol. Lett. 189 (2000) 165–169.

[22] T. Uchida, Y. Shibata, An affinity adsorbent, 5'-adenylate-aminohexyl-sepharose. I. Purification and properties of two forms of RNase U2. J. Biochem. 90 (1981) 463-471.

[23] S. Noguchi, Y. Satow, T. Uchida, C. Sasaki, T. Matsuzaki, Crystal structure of *Ustilago sphaerogena* ribonuclease U2 at 1.8 A resolution. Biochemistry 34 (1995) 15583–15591.

[24] J.M. Mancheño, M. Gasset, J. Lacadena, A. Martínez del Pozo, M. Oñaderra, J.G. Gavilanes, Predictive study of the conformation of the cytotoxic protein α-sarcin: a structural model to explain α-sarcin-membrane interaction. J. Theor. Biol. 172 (1995) 259–267.

[25] S. Sato, T. Uchida, The disulfide bridges of ribonuclease U2 from *Ustilago sphaerogena*. J. Biochem. 77 (1975) 1171-6.

[26] J. Sambrook, D.W. Russell, Molecular Cloning: A. Laboratory Manual 3rd edn. Cold Spring Harbor Laboratory, Cold Spring Harbor, New York, 2001.

[27] J. Lacadena, A. Martínez del Pozo, J.L. Barbero, J.M. Mancheño, M. Gasset, M. Oñaderra, C. López-Otín, S. Ortega, J.L. García, J.G. Gavilanes, Overproduction and purification of biologically active native fungal α-sarcin in *Escherichia coli*. Gene 142 (1994) 147-151.

[28] J. Lacadena, A. Martínez del Pozo, A. Martínez-Ruiz, J.M. Pérez-Cañadillas, M. Bruix, J.M. Mancheño, M. Oñaderra, J.G. Gavilanes, Role of histidine-50, glutamic acid-96, and histidine-137 in the ribonucleolytic mechanism of the ribotoxin α-sarcin. Proteins 37 (1999) 474-484.

[29] G.F. Vovis, S. Lacks, Complementary action of restriction enzymes endo R-DpnI and Endo R-DpnII on bacteriophage f1 DNA. J. Mol. Biol.115 (1977) 525-538.

[30] L. García-Ortega, M. Masip, J.M. Mancheño, M. Oñaderra, M.A. Lizarbe, M.F. García-Mayoral, M. Bruix, A. Martínez del Pozo, J.G. Gavilanes, Deletion of the NH2-terminal β-hairpin of the ribotoxin α-sarcin produces a nontoxic but active ribonuclease. J. Biol. Chem. 277 (2002) 18632–18639.

[31] A. Martínez-Ruiz, A. Martínez del Pozo, J. Lacadena, J.M. Mancheño, M. Oñaderra, C. López-Otín, J.G. Gavilanes, Secretion of recombinant pro- and mature fungal α-sarcin ribotoxin by the methylotrophic yeast *Pichia pastoris*: the Lys-Arg motif is required for maturation. Protein Expr. Purif. 12 (1998) 315–322.

[32] K.L. Hsi, L. Chen, D.H. Hawke, L.R. Zieske, P.M. Yuan, A general approach for characterizing glycosylation sites of glycoproteins. Anal. Biochem. 198 (1991) 238-245.

[33] E. Batanero, M. Villalba, R. Rodríguez, Glycosylation site of the major allergen from olive tree pollen. Allergenic implications of the carbohydrate moiety. Mol. Immunol. 31 (1994) 31-37.

[34] J.G. Gavilanes, D. Vázquez, F. Soriano, E. Méndez, Chemical and spectroscopic evidence on the homology of three antitumor proteins: α-sarcin, mitogillin, and restrictocin. J. Protein Chem. 2 (1983) 251–261.

[35] W.J. Becktell, J. A. Schellman, Protein stability curves. Biopolymers 26 (1987) 1859–1877.

[36] A. Blank, R.H. Sugiyama, C.A. Dekker, Activity staining of nucleolytic enzymes after sodium dodecyl sulfate-polyacrylamide gel electrophoresis: use of aqueous isopropanol to remove detergent from gels. Anal. Biochem. 120 (1982) 267-275.

[37] J.M. García-Segura, M.M. Orozco, J.M. Fominaya, J.G. Gavilanes, Purification, molecular and enzymic characterization of an acid RNase from the insect *Ceratitis capitata*. Eur. J. Biochem. 158 (1986) 367-372.

[38] L. García-Ortega, J. Lacadena, J.M. Mancheño, M. Oñaderra, R. Kao, J. Davies, N. Olmo, A. Martínez del Pozo, J.G. Gavilanes, Involvement of the amino-terminal β-hairpin of the *Aspergillus* ribotoxins on the interaction with membranes and nonspecific ribonuclease activity. Protein Sci. 10 (2001) 1658-1668.

[39] J. Steyaert, K. Hallenga, L. Wyns, P. Stanssens, Histidine-40 of ribonuclease T1 acts as base catalyst when the true catalytic base, glutamic acid-58, is replaced by alanine. Biochemistry 29 (1990) 9064-9072.

[40] J.L. Cereghino, J.M. Cregg, Heterologous protein expression in the methylotrophic yeast *Pichia pastoris*. FEMS Microbiol. Rev. 24 (2000) 45-66.

[41] J.M. O'Leary, C.M. Radcliffe, A.C. Willis, R.A. Dwek, P.M. Rudd, A.K. Downing, Identification and removal of O-linked and non-covalently linked sugars from recombinant protein produced using *Pichia pastoris*.Protein Expr. Purif. 38 (2004) 217-227.

[42] R. Koradi, M. Billeter, K. Wüthrich, MOLMOL: a program for display and analysis of macromolecular structures. J. Mol. Graph. 14 (1996) 51-55.

Figure 1. Representation of the structures and active site residues of RNase T1 and RNase U2. The images were generated with the MOLMOL program [42] from the atomic coordinates deposited in PDB (entries 1rnt and 1rtu, respectively). Superposition of side-chain residues corresponding to the active site of both RNase T1 (black) and RNase U2 (grey) is also represented. Numbers within brackets correspond to RNase U2.

Figure 2. Electrophoretic analysis. (A) SDS-PAGE and (B) Western blot of wild-type RNase U2 (1) and its C1/54S (2) and H101Q (3) mutants. All samples were boiled in the presence of 5.0% β-mercaptoethanol before being loaded onto the gel.

Figure 3. (A) SDS-PAGE and (B) zymogram against poly(A), at pH 4.5, of wild-type RNase U2 (1) and its C1/54S (2) and H101Q (3) mutants. Prior to be applied on the gel, all samples were boiled but in the absence of β-mercaptoethanol. (C) Biotinylated-Con A staining of a Western blot where the equivalent samples had been electrotransferred. In this case, samples were reduced with 5.0% β-mercaptoethanol before being loaded onto the polyacrylamide gel. The first line on the left corresponds to pre-stained *Precision Plus Protein*^{TM} Standard (BioRad)

Figure 4. Scheme showing the different signal peptide cleavage processing sites found for the different recombinant proteins studied according to their amino-terminal amino acid sequences.

Figure 5. Maldi-TOF analyses of wild-type RNase U2 and its mutants C1/54S and H101Q.

Figure 6. Spectroscopic characterization. (A) Far-UV circular dichroism spectra of wild-type (●), C1/54S (○), and H101Q (◍) recombinant versions of RNase U2 (B) Thermal denaturation profiles at pH 4.5 for wild-type RNase U2 (black) and its mutant C1/54S (grey) measured by recording the ellipticity

change at 220nm (Θ_{220}) vs temperature. Mean residue weight ellipticity ($[\Theta]_{MRW}$ or Θ_{220}) is expressed in deg cm^2 $dmol^{-1}$.

Figure 7. Fluorescence emission spectra of wild-type RNase U2 and the mutants C1/54S and H101Q. All spectra were recorded using proteins with identical 280 nm-absorbance values. Spectra labeled '1' resulted from excitation at 275 nm and spectra labeled '2' from excitation at 295 nm (tryptophan contribution). These spectra were normalized at wavelengths above 380 nm. Spectra '3' (tyrosine contribution) were calculated by subtracting spectra '2' from spectra '1'. Fluorescence emission units were arbitrary.

Table 1. Mutagenic primers used to construct the RNase U2 mutants H101Q and C1/54S. The bases that change the original codon are underlined.

mutation	oligonucleotide sequence
C1S forward	5'- AAA AGA GAG GCT GAA GCT GAA TTG T<u>C</u>C GAC ATC CCT CAG TCC ACC AAC TGC -3'
C1S reverse	5'- GCA GTT GGT GGA CTG AGG GAT GTC G<u>G</u>A CAA TTC AGC TTC AGC CTC TCT TTT -3'
C54S forward	5'- GAA GCG TCT GAA GAC ATT ACT CTT T<u>C</u>C TGT GGA TCC GGT CCT TGG TCC GAA -3'
C54S reverse	5'- TTC GGA CCA AGG ACC GGA TCC ACA G<u>G</u>A AAG AGT AAT GTC TTC AGA CGC TTC -3'
H101Q forward	5'- GGA GAG TTT TGT GCA ACC GTC ACT CA<u>A</u> ACG GGT GCA GCT AGT TAT GAC GGC -3'
H101Q reverse	5'- GCC GTC ATA ACT AGC TGC ACC CGT <u>T</u>TG AGT GAC GGT TGC ACA AAA CTC TCC -3'

Table 2. - Purification yields and structural features of the different RNase U2 protein versions studied.

Protein	yield[a]	$E^{0.1\%}$ (280 nm, 1 cm)	Tm (ºC) pH 4.5	Tm (ºC) pH 7.0	NH_2-terminal sequence
WT[b]	0.95	1.80	61	50	Glu-Ala-Glu
H101Q	0.71	n.d.[c]	n.d.[c]	n.d.[c]	Glu-Ala-Glu Glu-Leu-Cys Ala-Glu-Ala
C1/54S	0.78	1.74	50	42	Glu-Leu-Ser

[a]expressed as mg of protein isolated by liter of original yeast culture.

[b][19]

[c]not determined

Figure
Click here to download high resolution image

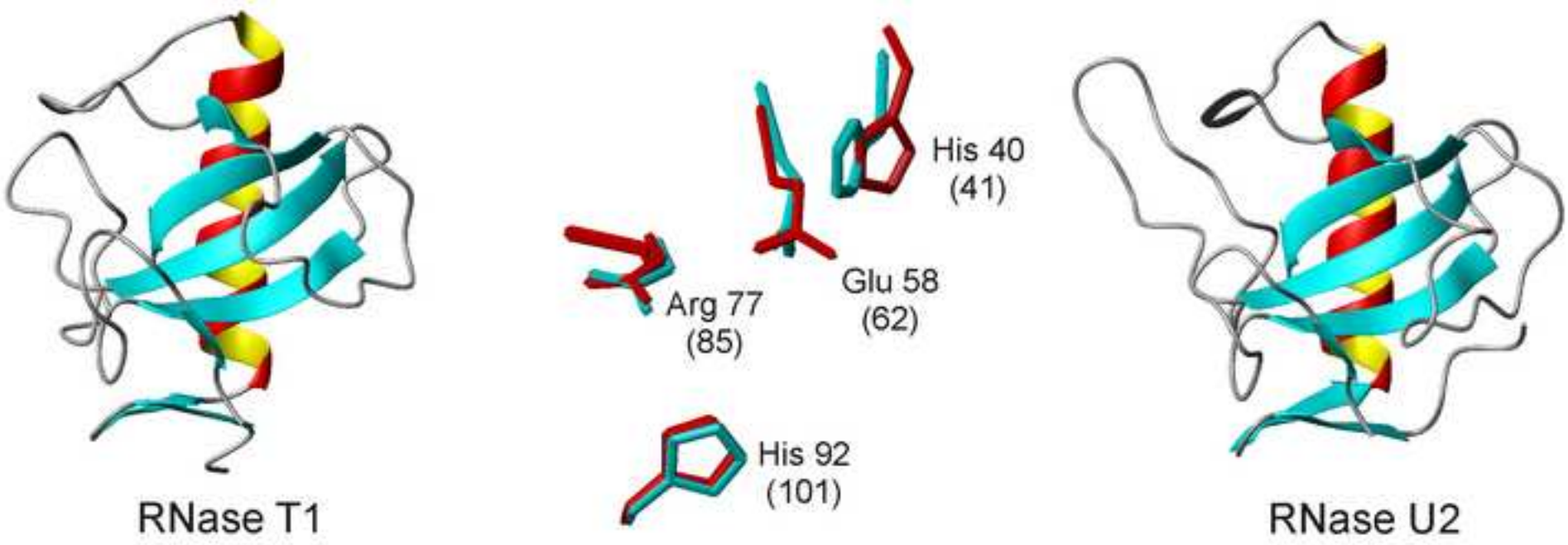

Figure

Click here to download high resolution image

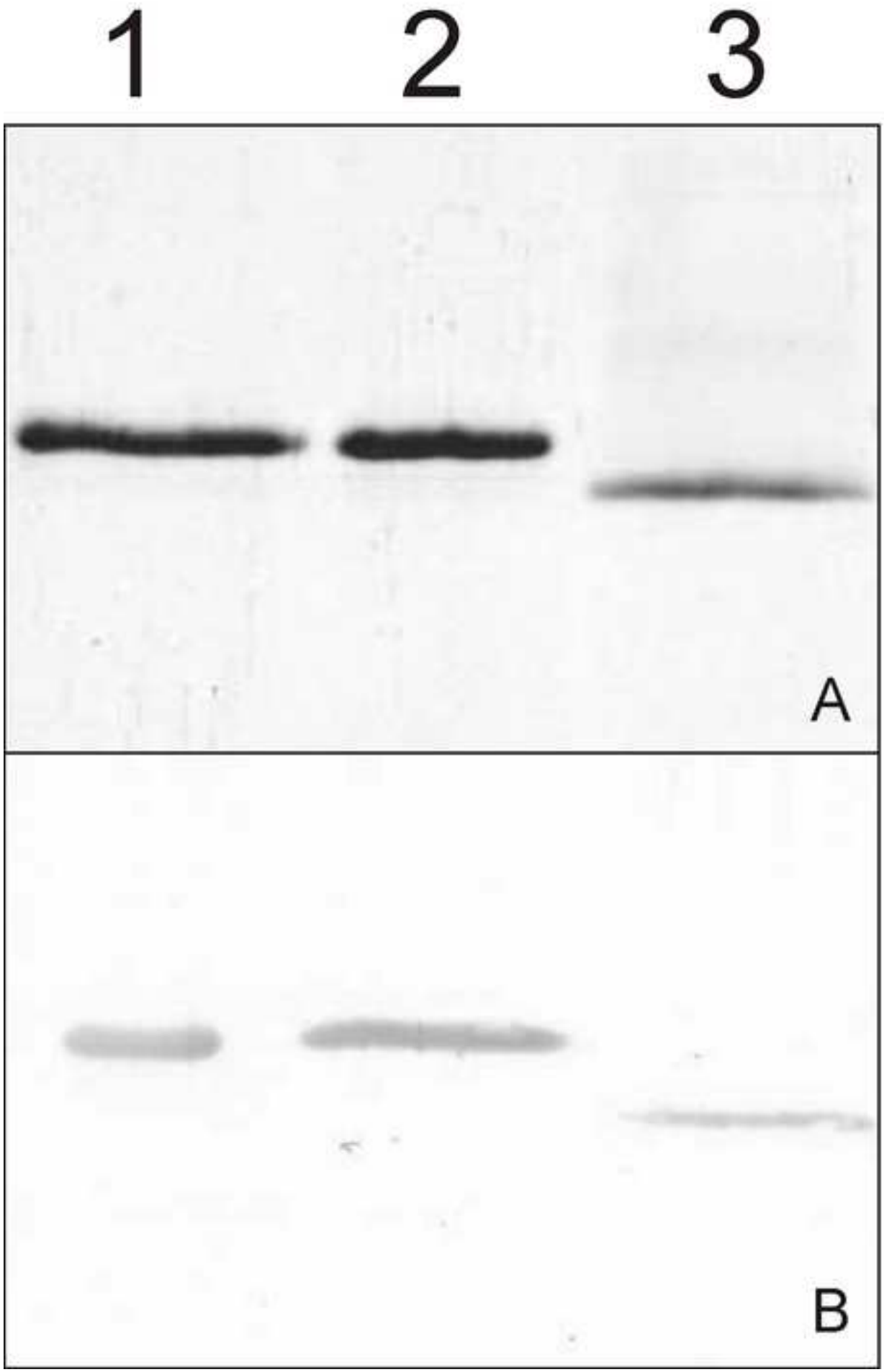

Figure

Click here to download high resolution image

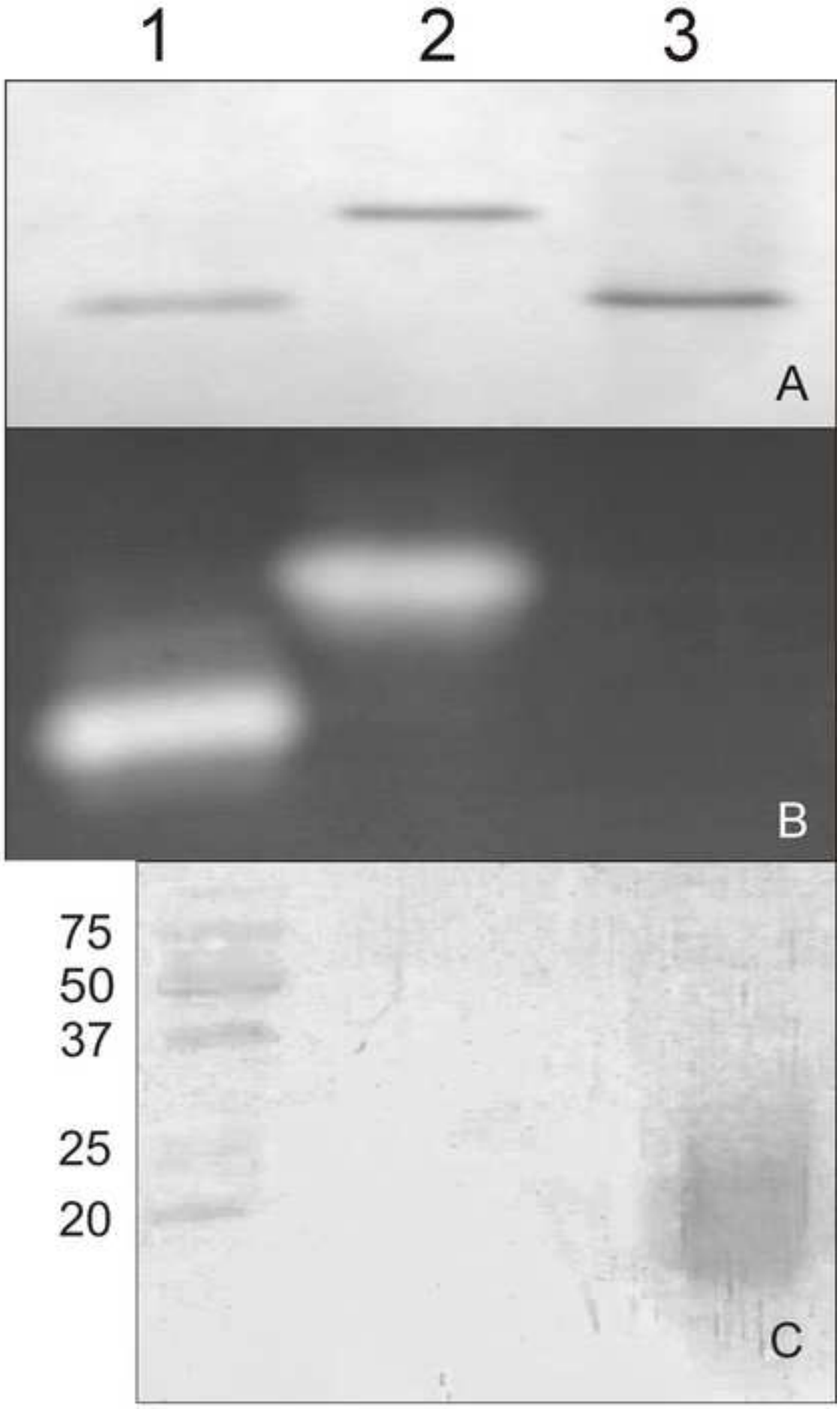

Figure
Click here to download high resolution image

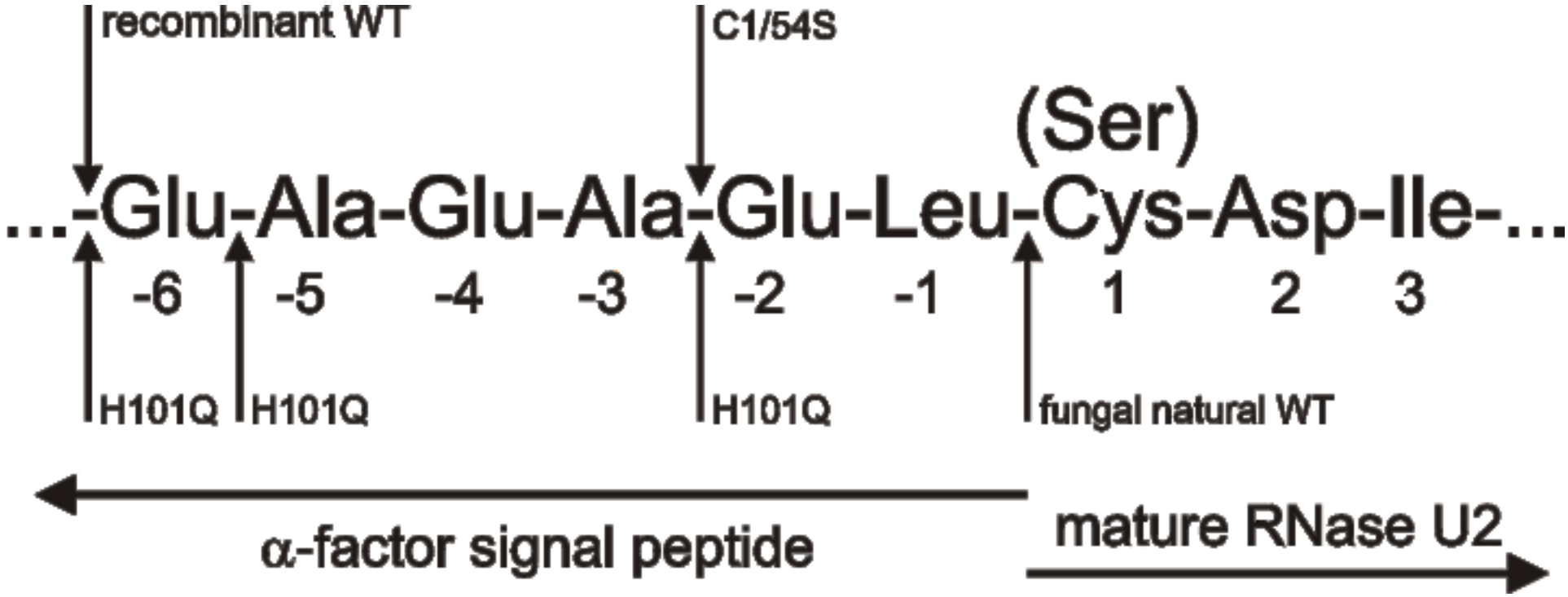

Figure

Click here to download high resolution image

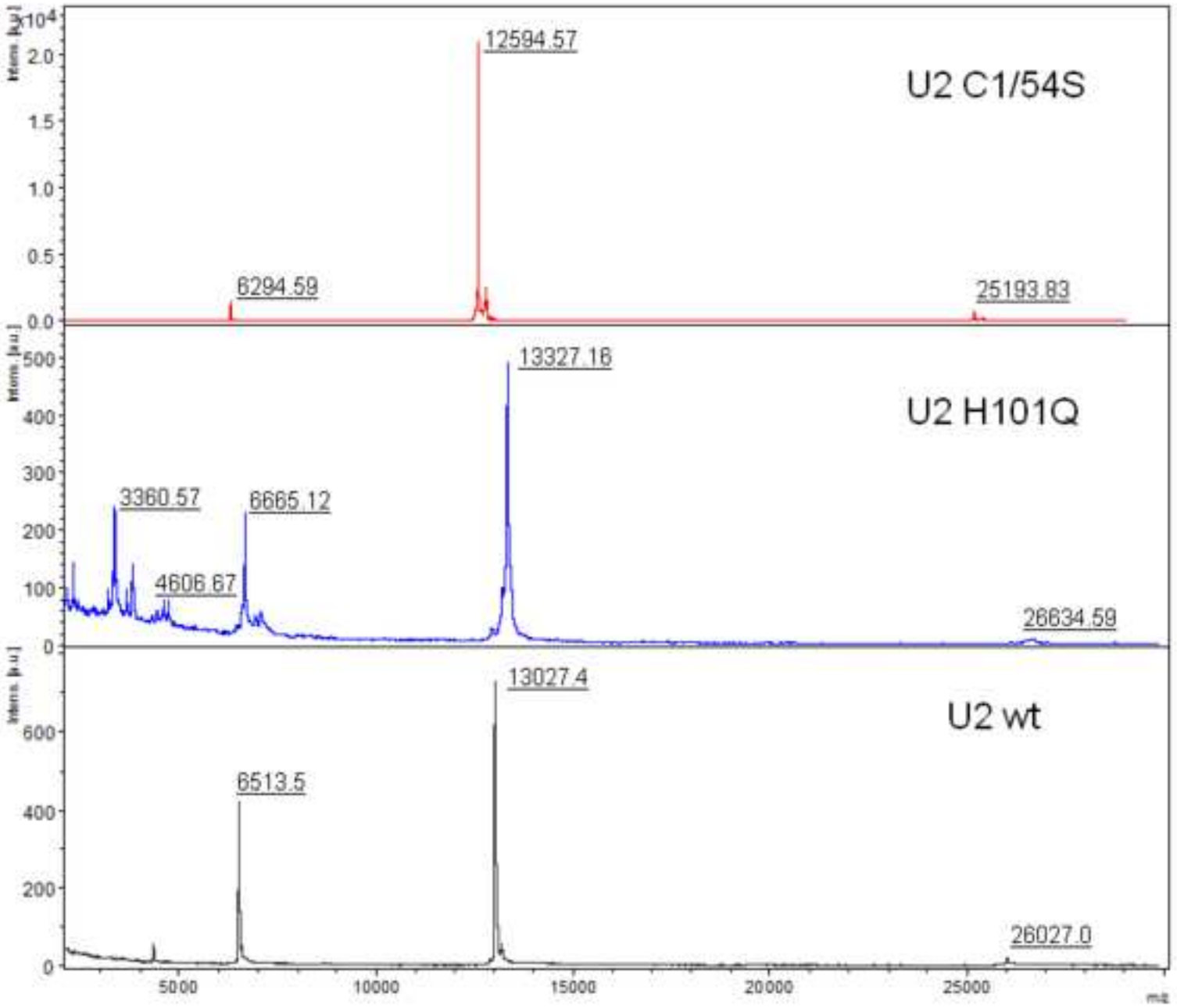

Figure

Click here to download high resolution image

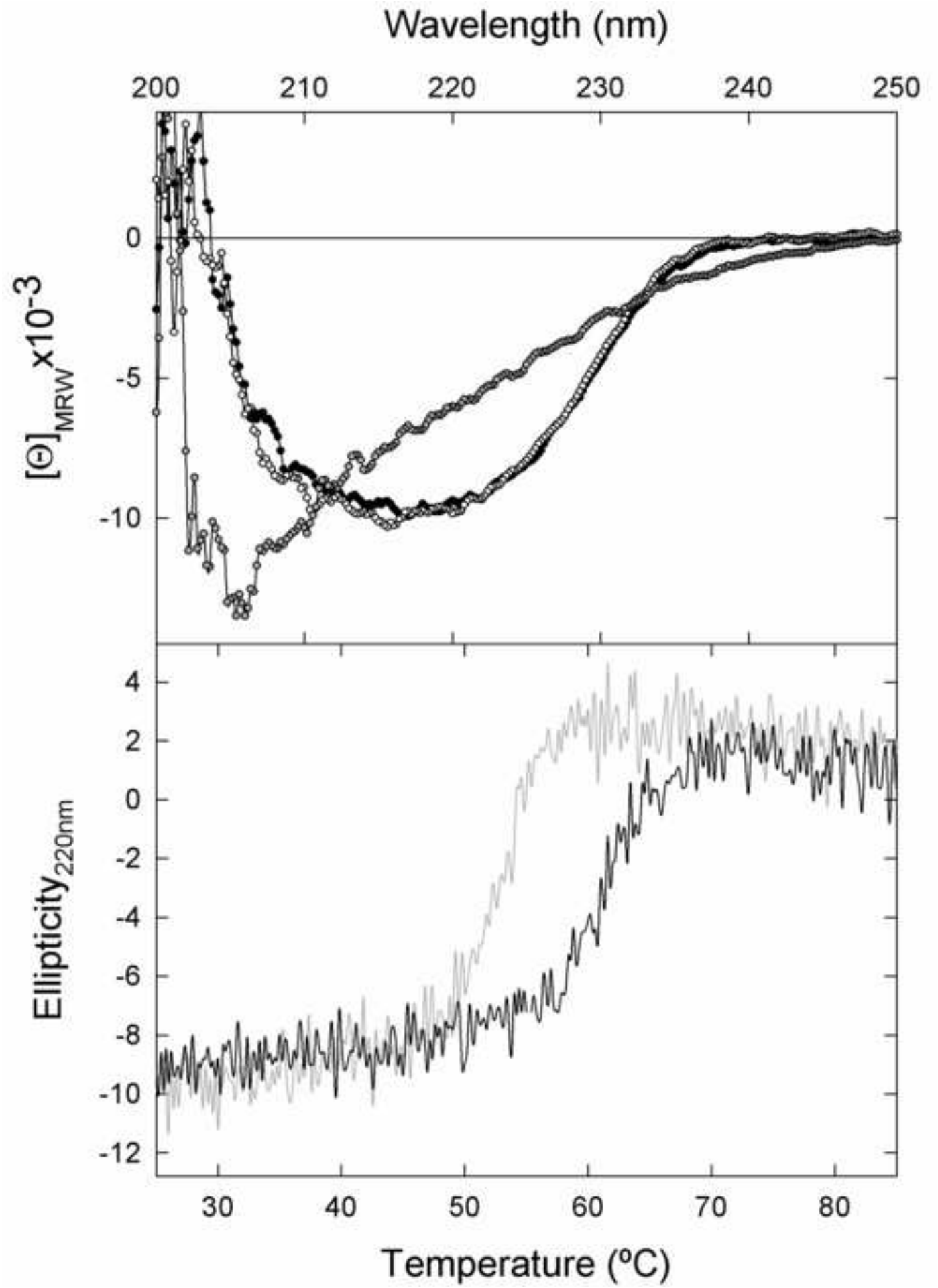

Figure

Click here to download high resolution image